Applied Energy 191 (2017) 358–366

Contents lists available at ScienceDirect

Applied Energy

journal homepage: www.elsevier.com/locate/apenergy

# The effects of flake graphite nanoparticles, phase change material, and film cooling on the solar still performance

S.W. Sharshir [a,b,c,1], Guilong Peng [a,b,1], Lirong Wu [a,b], F.A. Essa [c], A.E. Kabeel [d], Nuo Yang [a,b,*]

[a] State Key Laboratory of Coal Combustion, Huazhong University of Science and Technology, Wuhan 430074, China
[b] Nano Interface Center for Energy (NICE), School of Energy and Power Engineering, Huazhong University of Science and Technology, Wuhan 430074, China
[c] Mechanical Engineering Department, Faculty of Engineering, Kafrelsheikh University, Kafrelsheikh, Egypt
[d] Mechanical Power Engineering Department, Faculty of Engineering, Tanta University, Tanta, Egypt

## HIGHLIGHTS

- Four modifications on the solar still have been performed in this paper.
- Flake graphite nanoparticles, phase change material, and film cooling were combined.
- The effect of the water depth on the enhancement of productivity was studied.
- The mechanism of the enhancement by flake graphite nanoparticles was discussed.

## ARTICLE INFO

*Article history:*
Received 5 September 2016
Received in revised form 23 January 2017
Accepted 27 January 2017

*Keywords:*
Flake graphite
Nanoparticles
Solar still
Phase change material
Film cooling

## ABSTRACT

Solar still is a cheap and convenient device for producing freshwater, but it's not popular due to its low productivity. In this paper, we modified the conventional solar still. The outdoor performance of modified solar stills was studied to assess its potential for real application. The modifications include using flake graphite nanoparticles (FGN), phase change material (PCM), and film cooling. In the presence of the three previous modifications, the productivity was enhanced as high as 73.8% compared with that of the conventional still. The effect of water depth on the enhancement was also investigated. It shows that the enhancement of productivity increases by around 13% when the water depth decreases from 2 cm to 0.5 cm. Besides, an indoor experiment was carried out to analyze the enhancement mechanism by FGN. It shows that the increase in both temperature and saturated vapor pressure contributed to the enhancement.



## 1. Introduction

In the last few decades, fresh water scarcity has become more and more serious due to the increasing world population, excessive waste and growing pollution of natural water sources [1]. By 2025, there will be a big problem in water vulnerability for more than half of the world population [2]. Hence, people have to use efficient methods to produce freshwater. Solar still desalination is one of these methods. Solar still is a device having the advantages of easily fabricating, cheap, no specific skills to operate, approximately no maintenance and no need of conventional energy. However, on the other hand, it's not popular due to the low efficiency and low productivity.

Many works have been done to improve the performance of solar stills, mainly from three aspects: improving the structure, using special materials or using auxiliary equipment. such as plastic water purifier [3], regenerative desalination unit [4], greenhouse type solar still with mirrors [5]; modifying the solar still by reflector [6] or flat plate collectors [7,8]; changing the thickness of insulation [9]; wick type still [10], triple-basin still [11], capillary film still [12], multi effect still [13]; integrating the still with solar water collector [14], increasing the area of condensation surface [15]; using black gravel or black rubber [16], dye [17], and sponge cubes in the still [18]; double slope solar still[19]; modifying still by electrical blower [20], baffle suspended absorber [21], energy storing and wick materials [22,23]; and hybrid (PV/T) active still [24].

* Corresponding author at: Nano Interface Center for Energy (NICE), School of Energy and Power Engineering, Huazhong University of Science and Technology, Wuhan 430074, China.
*E-mail address:* nuo@hust.edu.cn (N. Yang).
[1] S.W.S. and G.P. equally contributed in this work.

http://dx.doi.org/10.1016/j.apenergy.2017.01.067
0306-2619/

Besides the modifications we mentioned above, researchers also found that the productivity can be increased by increasing the temperature difference between the water surface and inner surface of the glass cover. The difference can be kept up at a high value by using high cooling film flow rate and low cooling film temperature [25–28]. Meanwhile, many researchers have used phase change material (PCM) as an improving parameter of desalination system [29]. The effect of using latent heat thermal energy storage system (LHTESS) through two cascade stills was investigated by Tabrizi et al. [30]. Results obtained that the output of the basin still with LHTESS is slightly lower in a sunny day but higher in a cloudy day than that of the still without LHTESS. The mathematical study of a still with and without PCM was carried out by Dashtban and Tabrizi [31]. The daily output reached 6.7 and 5.1 kg/m$^2$ with and without PCM, respectively. Ansari et al. [32] examined a still incorporated with a PCM under the basin plate. The results show that the heat energy storage enhances significantly both the productivity of the fresh water and the efficiency of the distillation system.

Recently, with the development of nanotechnology, nanoparticle has attracted the attention of many researchers in solar desalination area. Normally, researchers using nanoparticles in solar still by making nanofluid. Nanofluid has a lot of special properties compared to its base liquid such as high thermal conductivity [33–40], high solar radiation absorptivity [41], which are helpful parameters to improve the productivity of stills. Nijmeh et al. [42] studied the efficiency of the solar still when using a violet dye, the results showed that the efficiency was enhanced by 29%. Elango et al. [43] examined an experimental study to increase the productivity of the still by using various nanofluid. The productivity of the still is improved by 29.95% when using the aluminum oxide ($Al_2O_3$) nanofluid, while the productivities of the solar stills with tin oxide ($SnO_2$) and zinc oxide (ZnO) nanofluid are 18.63% and 12.67% higher than that without nanofluid, respectively.

Kabeel et al. [44] studied the effects of aluminum oxide nanoparticles, vacuum and external condenser on the solar still performance. Results showed that the daily productivity can be increased by 53.2% when the still was provided vacuum inside and the daily productivity can be increased by 116% when the still was provided vacuum inside and added aluminum oxide nanoparticles at the same time. Sahota and Tiwari [45] conducted an experimental and theoretical study to improve the productivity of a double slope solar still (DSSS) by using $Al_2O_3$ nanoparticles. The productivity of DSSS with aluminum oxide ($Al_2O_3$) nanofluid was improved by 12.2% and 8.4% at 35 kg and 80 kg base fluid respectively, with 0.12% concentration of $Al_2O_3$ nanoparticles.

From the above literature review, it is observed that the effect of using either some new nanoparticle or coupling the nanoparticle with PCM and film cooling are not investigated. In this paper, the flake graphite nanoparticles (FGN) were chosen as the nanomaterial in consideration of its relative high thermal conductivity [46,47], low cost and high solar absorptivity as compared with most of the nanomaterials. Hence, the major target of this work is to enhance the solar still performance by: (A) mixing the FGN with water, (B) mixing the FGN with water and placing encapsulated PCM (paraffin wax in this paper) on basin liner, (C) mixing the FGN with water and using film cooling on glass cover, and (D) mixing the FGN with water, placing encapsulated PCM on basin liner and using film cooling on glass cover.

It should be noted that, for all the modifications, the FGN were simply mixed with water manually without any additives. Most of the particles were deposited on the basin liner during the experiment procedure instead of stable suspended in the water. The large specific surface area of FGN increases the contact area with water, which contributes to a good heat transfer between FGN and water. When the water-FGN mixture (WFGN) is heated, some of the deposited particles flow up and down with water convection due to the relatively low density and small size. Meanwhile, a part of FGN aggregate at the triple phase contact line of the still due to the surface tension and water convection. Compared with making stable nanofluid in other works, the way to use FGN in this paper needs lower technique level and cost, which is highly acceptable in practical application. Besides, the particles can be easily recycled by filtering with cloth due to its relative large lateral size.

## 2. Experimental setup

The solar stills and all components of the system were manufactured in the school of energy and power engineering, Huazhong university of science and technology, Wuhan, China (Latitude 30°51′N and longitude 114°41′E).

Four modifications named modification (A), (B), (C) and (D) were designed in this paper. For modification (A), at first, 0.5% mass concentration of FGN was mixed with the water by shaking and stirring manually to make WFGN. Then the black WFGN was poured into the solar still through the drain hole of the still. Most of the particles deposited in dozens of minutes. The average lateral size of the FGN is around 1.3 μm, the thickness of the FGN is around 100 nm. The SEM image of the particles is shown in Fig. 3a.

For modification (B), apart from the 0.5% mass concentration FGN, 20 stainless steel pipes with PCM encapsulated inside were put on the basin liner to store the energy. Each pipe is 49 cm in length and 1.6 cm in diameter. The outer surfaces of the pipes were painted black to absorb more solar energy. The specifications of FGN and PCM are shown in Table 1.

Modification (C) added the film cooling on the basis of modification (A). The film cooling means some cold water was flow on the upper surface of the glass cover to cool down the glass cover. The mass flow rate of the cooling film in modification (C) was fixed at about 0.03 kg/s which was measured by collecting the cooling water. A cold water tank with the dimensions of 88 × 42 × 42 cm was used to supply the cooling water. The cooling water flowed out from the holes of a plastic pipe which was connected to the tank.

Modification (D) combined the 0.5% mass concentration FGN, 20 pipes with PCM encapsulated inside and the 0.03 kg/s film cooling all together. It's the union of the modification (A), (B), and (C). If not stated, the water depth in solar stills for all modifications is 0.5 cm.

The experiment system consists of three solar stills. A photograph and a schematic graph of the solar desalination setup are shown in Figs. 1 and 2, respectively. During the experiment procedure, one of the three solar still was used to work as a conventional solar still, and the other two were used to work as the modified solar stills. The area of the still basin is 0.25 m$^2$ (0.5 m length × 0.5 m width). The height of the low and high side wall is 160 mm and 450 mm, respectively. The stills are made of iron sheets (1.5 mm thick). The inner surface of the basin and the side walls of the solar stills were painted black to absorb the solar irradiation. To decrease the heat loss, all external surfaces were insulated by fiberglass (5 cm thickness). The thickness of the glass cover is 3.5 mm. The tilt angle of the glass cover is 30°. The system was kept in the south direction during the experiment process. A

**Table 1**
Specifications of FGN and PCM.

| Property | Value |
|---|---|
| Thermal Conductivity of FGN, (W/(m K) | 129 |
| Density of FGN, (g/cm$^3$) | ~2 |
| Lateral size of FGN, (μm) | ~1.3 |
| Thickness of FGN, (nm) | ~100 |
| Mass concentration of FGN in WFGN, (%) | 0.5 |
| Melting temperature of PCM, (°C) | 48 |

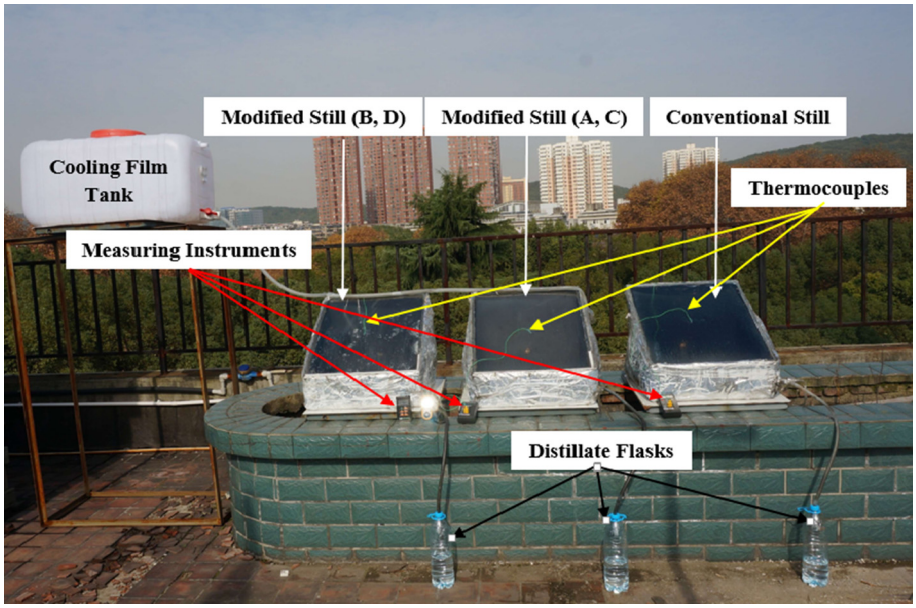


**Fig. 1.** Photograph of the experimental setup.

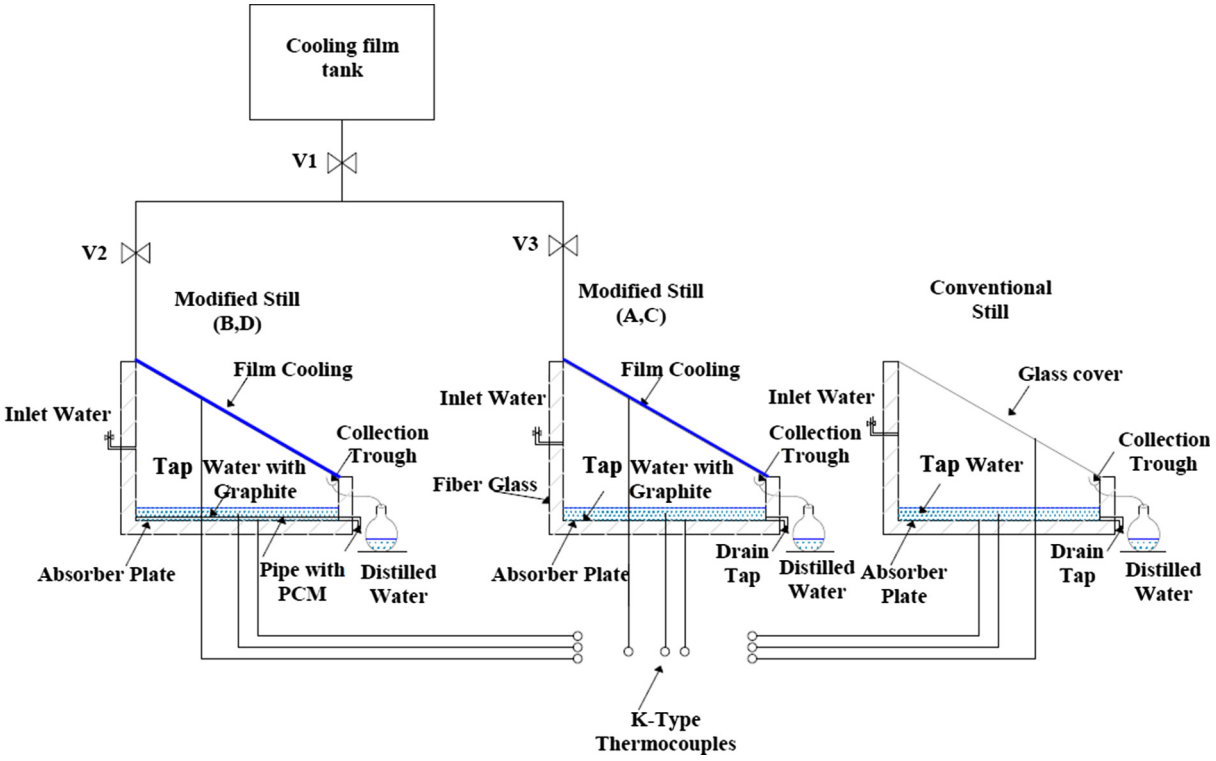


**Fig. 2.** Schematic graph of the experimental setup.

trough inside the still was used to collect the fresh water from the glass cover, a plastic pipe was connected to the trough for draining the water to an outside bottle. The brine was drained outside of the still through the drain hole by another pipe. The tap water is used to work as the sea water in this paper.

The uprising water vapor condensed on the inner surface of the glass cover. Due to the gravity and the tilting of the glass cover, the condensed water run down to the small inclined triangular channel (trough) to be collected into the bottle. Basically, the temperature of the ambient, brine and outer glass cover, the solar radiation, the wind velocity and the productivity of each still were measured every hour. The temperatures were measured by K type thermocouples with the range of (−50 to 180 °C) and accuracy of (±1 °C). While, a solar meter (TES-1333R, 0–2000 W/m$^2$, ±10 W/m$^2$) was used to measure the solar intensity. The wind velocity was measured by using a vane type digital anemometer (GM816) with the measuring range of (0.1–30 m/s) and the accuracy of ±0.1 m/s. The productivity was measured by a graduated cylinder (±2 ml). The uncertainty of the instruments and measurements are listed in Table 2.

**Table 2**
Uncertainty in measured parameters.

| Parameter | Uncertainty |
|---|---|
| Solar intensity | 10 w/m$^2$ |
| Length, width, diameter and thickness | 0.5 mm |
| Wind velocity | 0.1 m/s |
| Hourly productivity | 2 ml |
| Temperature by thermal couples | 1 °C |
| Temperature by IR camera | 1 °C |
| Mass change by balance | 0.0002 g |

The enhancement, $\varphi$, of productivity for modifications is calculated as:

$$\varphi_m = \frac{A_m \sum_{i=10}^{20} P^i_m - A_c \sum_{i=10}^{20} P^i_c}{A_c \sum_{i=10}^{20} P^i_c} \times 100\% \quad (1)$$

where $A$ is the area of basin, $P$ is the hourly productivity, the subscript $m$ means modified solar still, $c$ means the conventional solar still, the superscript $i$ means $i$ o'clock.

The total uncertainty, $S$, of the enhancement, $\varphi$, is propagated by the uncertainty of: the hourly productivity $P^i_m$, $P^i_c$, and the area $A_m$, $A_c$. It is calculated as:

$$S_\varphi = \sqrt{\left(\frac{\partial \varphi}{\partial \sum_{i=10}^{20} P^i_m}\right)^2 S^2_{\sum_{i=10}^{20} P^i_m} + \left(\frac{\partial \varphi}{\partial \sum_{i=10}^{20} P^i_c}\right)^2 S^2_{\sum_{i=10}^{20} P^i_c} + \left(\frac{\partial \varphi}{\partial A_m}\right)^2 S^2_{A_m} + \left(\frac{\partial \varphi}{\partial A_c}\right)^2 S^2_{A_c}} \quad (2)$$

Besides, to further discuss the enhancement mechanism, an indoor experiment was carried out to measure the detailed data of the temperature and evaporation. The schematic graph of the indoor experiment setup is illustrated in Fig. 4. The solar intensity was adjusted to 1 kw/m$^2$. The ambient temperature and humidity were controlled at 25 ± 0.5 °C and 60 ± 2%, respectively. The ambient wind velocity was close to 0 m/s.

## 3. Results and discussion

### 3.1. Effect of using FGN [modification(A)]

The absorption characteristics of the tap water, black painted basin, and WFGN were measured by UV–Vis spectrophotometer (LabRAM HR800) and shown in Fig. 3b. The absorption of WFGN is around 99.5%, which is about 5.5% higher than that of the black painted basin (94%). It is because of that the WFGN has a 3D absorbing structure, which is good for trapping the light to be absorbed for many times on the FGN surface.

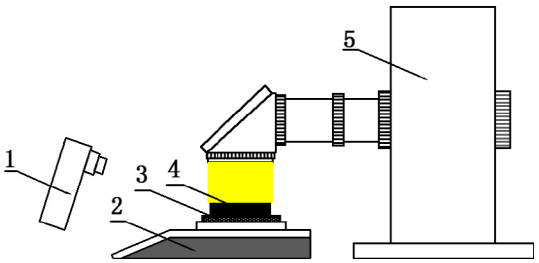


**Fig. 4.** The schematic graph of the indoor experiment setup. 1-IR camera (IRS S6, ±1 °C) to monitor the surface temperature; 2-balance (Sartorius Practum 224, ±0.0002 g) to measure the mass change; 3-polystyrene insulation (k = 0.036 W/(m K)), the thickness is 1 cm; 4-black painted stainless steel culture dish with fluid depth at 1 cm; 5-solar simulator (CEL-S500R) to generate the solar light.

Due to the better absorption characteristic of WFGN and large heat transfer area between FGN and water, the water and glass temperatures of the still with modification (A) are higher than those of the conventional still by (0–4) °C and (0–2) °C, respectively, as shown in Fig. 5a. Therefore, compared with the conventional still, both of the water temperature and water–glass temperature difference of the still with modification (A) are higher as shown in Fig. 5e, which obviously contributes to the enhancement of productivity.

The hourly productivity of the still with modification (A) and the conventional still are shown in Fig. 5b. It can be found from the figure that the hourly productivity of the still with modification (A) is higher than that of the conventional still all the day. Consequently, with modification (A), the productivity of still enhances by about 50.3%. The enhancement is high compared with previous works which used various nanoparticles as illustrated in Table 3. Meanwhile, it can be concluded from Fig. 5a, b that the trend of the productivity curves is similar to the trend of the temperature curves. This indicates that the temperature affects the productivity a lot.

### 3.2. Effect of using FGN and PCM [modification (B)]

The hourly temperature variations and solar radiation for the still with modification (B) and the conventional still are illustrated in Fig. 5c. And the hourly productivity variation for the still with modification (B) and conventional still is shown in Fig. 5d. It is also observed from the figures that the peaks of temperature and productivity curves of the still with modification (B) appeared after the peak of solar radiation curve. This is because that some of the heat inside the solar still were stored as the sensible and latent heat in the PCM and this needs longer time and more energy to rise

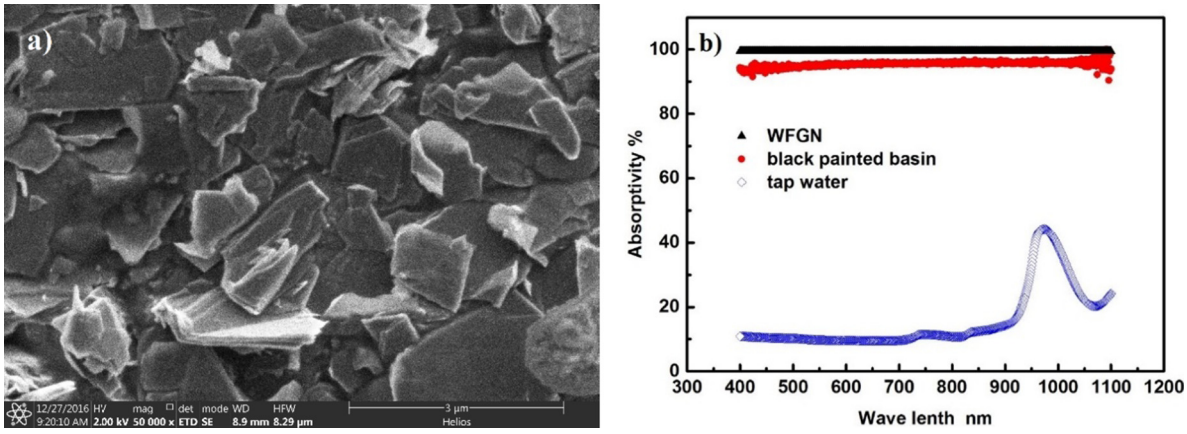


**Fig. 3.** (a) The SEM image of the graphite nanoparticles (the scale bar is 3 µm), (b) The absorptivity of the tap water, black painted basin and WFGN.

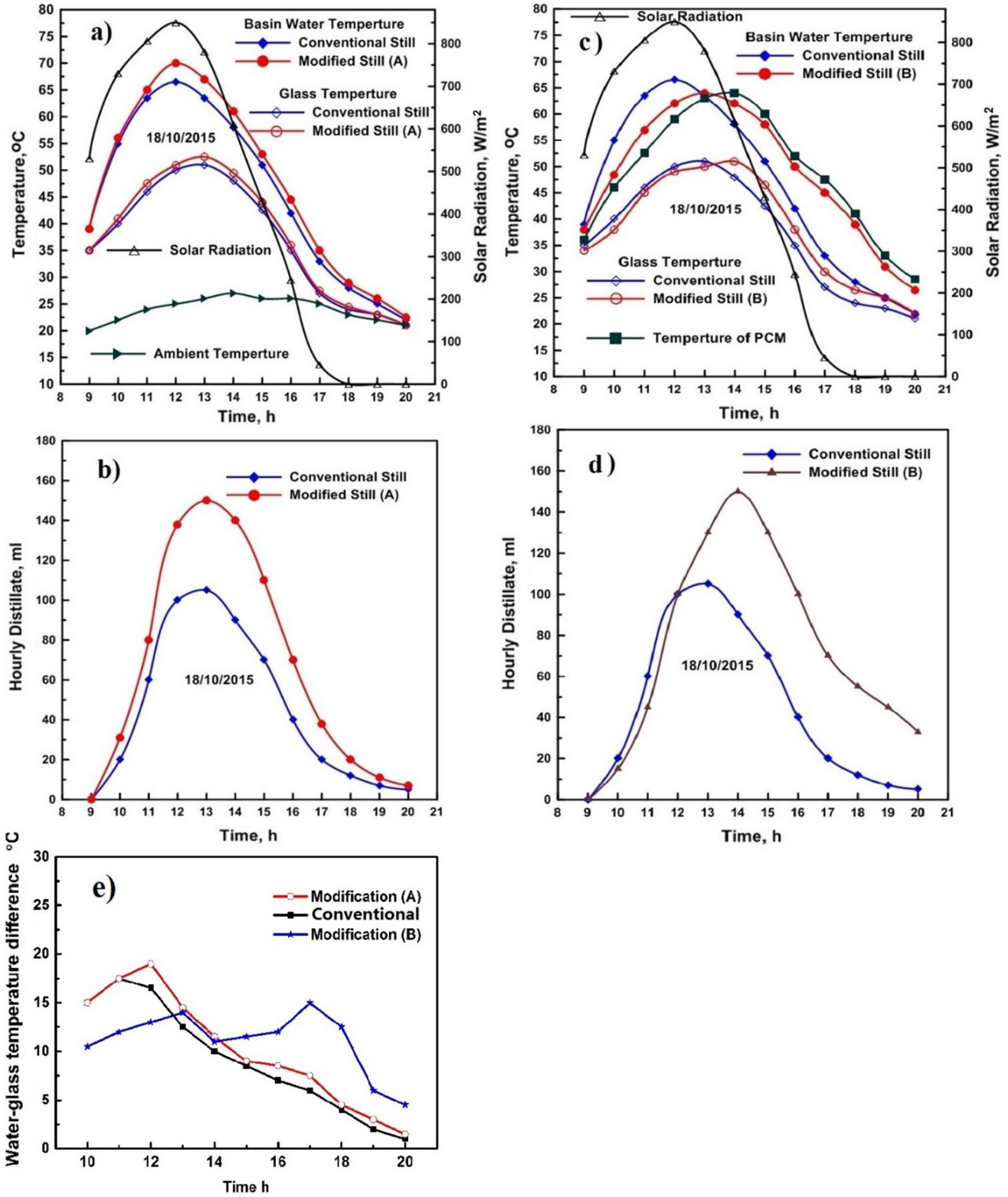


**Fig. 5.** Hourly variations of the solar radiation, basin water and glass temperatures, productivity and water–glass temperature difference for the modification (A), (B) and conventional stills. (a), (c). Solar radiation and temperatures. (b), (d). Fresh water productivities. (e) Water –glass temperature differences on 18/10/2015.

the temperatures. Therefore, the temperatures and productivity of the conventional still are higher from about 9:00 a.m. to 12:00o'clock as shown in Fig. 5c, d.

Meanwhile, it is obtained from Fig. 5c that, in the afternoon, the decrease of water temperature of the still with modification (B) is slower than that of the conventional still due to the PCM. Consequently, both of the water–glass temperature difference (shown in Fig. 5e) and water temperature of the still with modification (B) are higher after 13 p.m. Besides, the PCM has an obvious effect after sunset (around 18:00) as shown in Fig. 5d. For still with PCM

**Table 3**
Comparison between present study and various works about still with nanoparticles.

| References, location | Modification | Maximal. enhancement in productivity |
|---|---|---|
| Present study, Wuhan, China | Using FGN [modification (A); PCM and FGN [modification (B)]; FGN and film cooling [modification (C)]; FGN, PCM and film cooling [modification (D)] | 50.28%, modification (A) 65.00,%, modification (B) 56.15%, modification (C) 73.80%, modification (D) |
| Nijmeh et al. [42], Amman, Jordan | Using potassium permanganate: ($KMnO_4$) and potassium dichromate ($K_2Cr_2O_7$) | 26%, $KMnO_4$ 17%, $K_2Cr_2O_7$ |
| Elango et al. [43], Tamil Nadu, India | Using Aluminum Oxide ($Al_2O_3$), Iron Oxide ($Fe_2O_3$), Zinc Oxide (ZnO) nanoparticles | 29.95%, Aluminum Oxide 18.63%, Iron Oxide 12.67%, Zinc Oxide |
| Kabeel et al. [44], Kafrelsheikh, Egypt | Using aluminum-oxide nanoparticles and external condenser | 116%, aluminum-oxide with vacuum |
| Sahota and Tiwari [45] New Delhi, India | Using aluminum-oxide nanoparticles | 12.2%, aluminum oxide |

**Table 4**
Enhancement of productivity for the modified solar stills compared with the conventional still for various water depth.

| Modification | Water depth (cm) | Enhancement (%) |
|---|---|---|
| (A) | 0.5 | 50.3 ± 1.9 |
| | 1 | 45 ± 1.8 |
| | 2 | 37 ± 1.9 |
| (B) | 0.5 | 65 ± 2 |
| | 1 | 60.3 ± 1.9 |
| | 2 | 52 ± 1.9 |

(modification (B)), a considerable amount of fresh water is produced during the nighttime (18:00–20:00). In total, the daily productivity (from 9:00 to 20:00) reached approximately 873 ml/day which is 65% higher than that of the conventional solar still (529 ml/day).

Furthermore, Table 4 shows the effect of the water depth on modification (A) and modification (B). The results show that the lower the basin water depth, the higher output percentage for the tested two modifications. The enhancement of productivity increases by around 13% when the water depth decreases from 2 cm to 0.5 cm for both modification (A) and (B). Moreover, the enhancement of productivity for the still with modification (B) was higher than that of the still with modification (A) regardless of the water depth.

### 3.3. Effect of using FGN and film cooling [modification (C)]

According to Fig. 5a, the water temperature of the still with modification (A) is higher than that of the conventional still. However, the glass temperature is also higher than that of the conventional still due to the increased vapor amount. The water–glass temperature difference is limited by the increased glass temperature. As a result, the enhancement of productivity is limited. Therefore, the cooling film was used to catch some heat stored in the glass by conduction and convection to increase the water–glass temperature difference. Consequently, the glass temperature was cooled down to keep a high water–glass temperature difference as shown in Fig. 6e. Hence, the productivity was further increased. Besides, the cooling film can clean the glass cover to maintain a good solar transmittance of the glass cover.

The variation of the solar radiation, basin water, glass cover and ambient temperatures for the still with modification (C) and conventional still are shown in Fig. 6a. The hourly productivity variations for the still with modification (C) and conventional still are shown in Fig. 6b. From the figures, it is obvious that the glass cover temperature of still with modification (C) is less than that of conventional still by about 1–21 °C. Meanwhile, the water temperature decreased by 6 °C due to some energy was taken away by the cooling film. The water–glass temperature difference for the still with modification (C) increased by about 27 °C and is higher than that of the conventional still by 16 °C in the noon as shown in Fig. 6e. Consequently, the productivity of the still with modification (C) increased by 56.2% compared with the conventional still.

### 3.4. Effect of using FGN, PCM and film cooling [modification (D)]

The evaporation rate can be increased by using the PCM and FGN and the condensation rate can be increased by using the cooling film. Therefore, in this part, the performance of the solar still with PCM, FGN, and film cooling was investigated to show the overall effect. The hourly variations of temperatures of the water, glass cover, PCM and productivity are illustrated in Fig. 6c, d. It can be obtained from Fig. 6c that as the solar intensity increases the temperature of PCM also increases because of the increased heat transfer by conduction from the black metal pipes to the PCM. After 13:00, PCM started to discharge the stored heat and keep the water warmer than that of the conventional still.

Meanwhile, the glass temperature of the still with modification (D) is less than that of conventional solar still by around 1–22 °C due to the film cooling. As shown in Fig. 6e, the water–glass temperature difference for the still with modification (D) reached about 28 °C in the noon. Due to the combination of the film cooling and PCM, the water–glass temperature difference of the still with modification (D) is much higher than that of the conventional still all the day, which contributes a lot to the enhancement of productivity. The productivity of the still with modification (D) is enhanced by 73.8% compared with that of the conventional still. The enhancement of productivity for different modifications and different dates is summarized and listed in Table 5.

### 3.5. Detailed data of the temperature and evaporation

From the above discussion, we can know that the temperature is an important parameter for enhancing the productivity. However, according to Fig. 5a, there is also an enhancement (around 30%) of modification (A) in the morning (9–11 a.m.), when the temperatures of the still with modification (A) are almost the same as that of the conventional still. To further study the phenomenon and analyze the mechanism, an indoor experiment was carried out to measure the detailed data of the temperature and evaporation.

As illustrated in Fig. 7a, the difference of the surface temperature between the tap water and WFGN is not obvious. In the beginning (0–300 s), the surface temperature of the WFGN is slightly higher than that of the tap water (less than 1 °C). After 300 s, the surface temperature of the water is almost the same as that of the WFGN. However, the evaporation rate of the WFGN is higher than that of the tap water all the time as illustrated in Fig. 7b. Fig. 7c shows the accumulated mass change of the tap water and WFGN and the enhancement by FGN. The enhancement is around 30%.

Obviously, the results of indoor and outdoor experiment are consistent. It can be explained by the increase in saturated vapor pressure. The relationship between the evaporation rate, $J^*_{eV}$, and the saturated vapor pressure of the liquid at the vapor–liquid

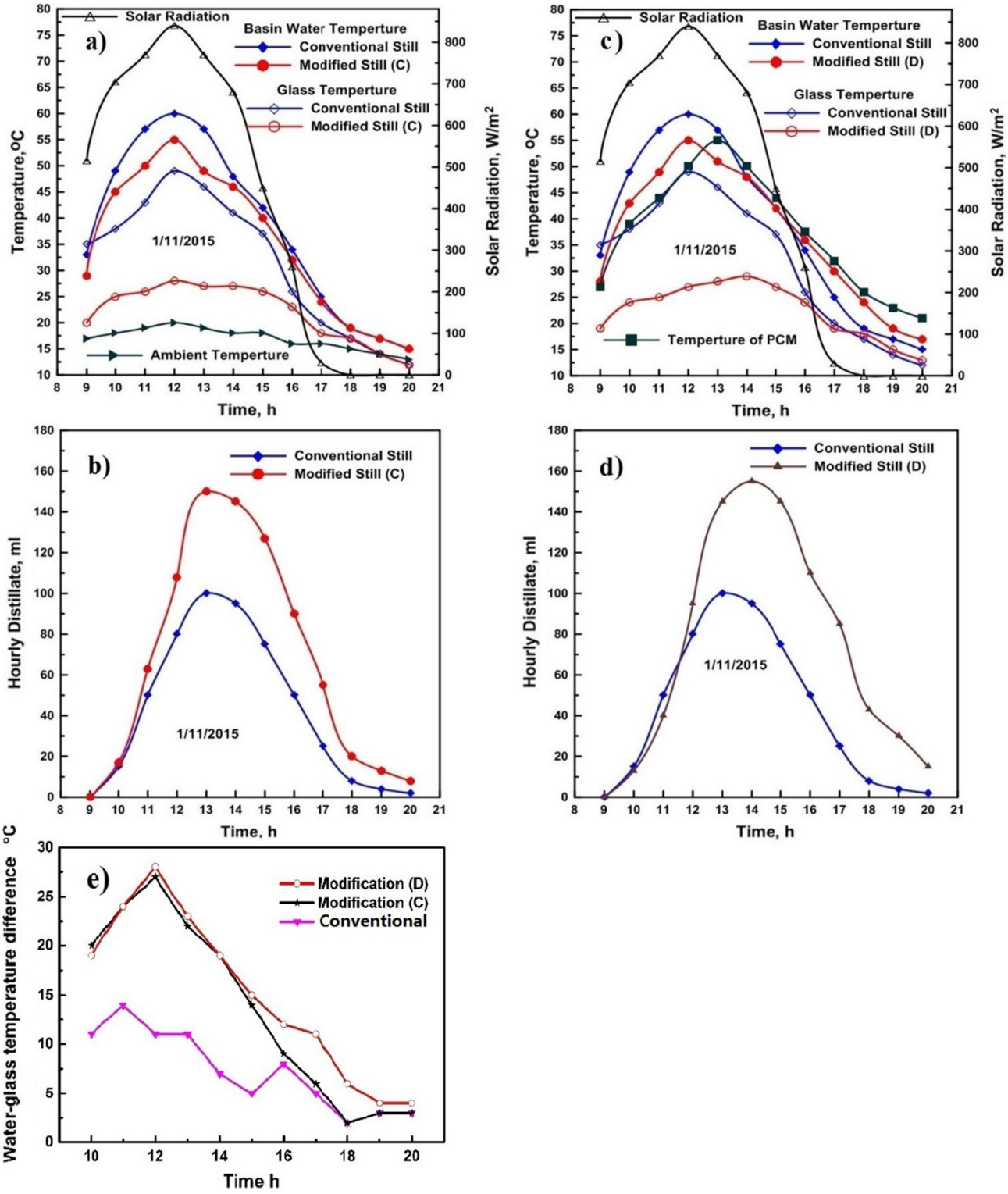


**Fig. 6.** Hourly variations of solar radiation, basin water and glass temperatures, productivity and water–glass temperature difference for the modification (C), (D) and conventional stills. (a), (c) Solar radiation and temperatures. (b), (d) Fresh water productivities. (e) Water –glass temperature differences on 1/11/2015.

interface, $P_{sL}$, can be described as TED-SRT evaporation flux expression [48]:

$$J_{eV}^{*} = \sqrt{\frac{m}{2\pi k_B}}\left(\sigma_e^{*}\frac{P_{sL}}{\sqrt{T_L}} - \sigma_c^{*}\frac{P_V}{\sqrt{T_V}}\right) \tag{3}$$

where $m$ is the mass of a molecule, and $k_B$ is the Boltzmann constant. $T_L$ is the temperature of the liquid at the vapor–liquid interface, $P_V$ and $T_V$ are the real vapor pressure and temperature of the vapor at the vapor–liquid interface, respectively. $\sigma_e^{*}$ and $\sigma_c^{*}$ are the evaporation coefficient and condensation coefficient, respectively:

$$\sigma_e^{*} \equiv \frac{P_{sL}}{P_V}\exp\left[(DOF+4)\left(1-\frac{T_V}{T_L}\right)\right]\left(\frac{T_V}{T_L}\right)^{DOF+4} \tag{4}$$

**Table 5**
The enhancement of productivity for modifications on different date.

| Date | Modification | Enhancement, φ, (%) |
|---|---|---|
| 16/10/2015 | (A) | 49 ± 1.9 |
| | (B) | 64.7 ± 1.9 |
| 18/10/2015 | (A) | 50.3 ± 1.9 |
| | (B) | 65 ± 2 |
| 26/10/2015 | (C) | 55.8 ± 2 |
| | (D) | 71.4 ± 2.1 |
| 1/11/2015 | (C) | 56.2 ± 2 |
| | (D) | 73.8 ± 2.1 |

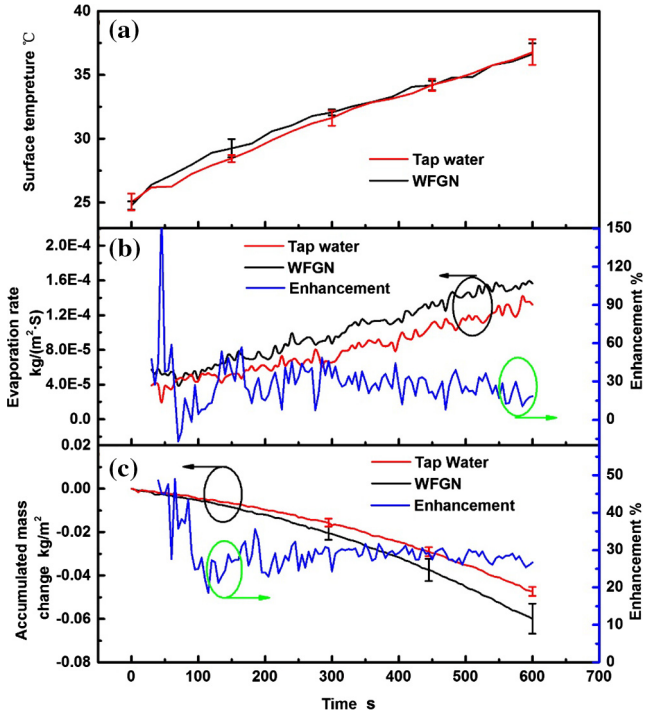


**Fig. 7.** Detailed data of the temperature and evaporation. (a) The average surface temperature of the tap water and WFGN. (b) The evaporation rate of the tap water and WFGN and the enhancement by FGN, (c) The accumulated mass change of the tap water and WFGN and the enhancement by FGN.

$$\sigma_c^* \equiv \sqrt{\frac{T_V}{T_L}} \exp\left[-(DOF+4)\left(1-\frac{T_V}{T_L}\right)\right]\left(\frac{T_V}{T_L}\right)^{DOF+4} \quad (5)$$

where DOF indicates the vibrational frequency degrees of freedom. The DOF values for nonlinear and linear molecules are 3n-6 and 3n-5, respectively, where n is the number of atoms in the molecule.

As observed, the temperature of the tap water and WFGN was the same. Therefore, the only driving force for a higher productivity is the higher $P_{sL}$. The increase in saturated vapor pressure is verified by Refs. [49,50]. Ref. [49] obtained that the evaporation rate and saturated vapor pressure are enhanced by adding nanoparticles in water. And the enhancement is affected by the material of nanoparticles. Meanwhile, Ref. [50] found that hydrophobic nanoparticles can obviously enhance the evaporation rate and saturated vapor pressure. Therefore, for all the modifications, the increase in both temperature and saturated vapor pressure of water contribute to the enhancement.

## 4. Conclusions

The simple mixing method for using FGN in solar stills was proven to be effective. The enhancement of productivity of the still with FGN [modification (A)], FGN and PCM [modification (B)], FGN and film cooling [modification (C)], FGN, PCM, and film cooling [modification (D)] are 50.28%, 65%, 56.15%, 73.8%, respectively. The enhancements are resulted from the higher water temperature by FGN and PCM, higher saturated vapor pressure of water by FGN, and higher water–glass temperature difference by film cooling. Meanwhile, the performance of solar stills decreases as the water depth increases for both modification (A) and modification (B).

## Acknowledgements

N.Y. was sponsored by the National Natural Science Foundation of China (No. 51576076).

## References

[1] Shannon MA, Bohn PW, Elimelech M, Georgiadis JG, Marinas BJ, Mayes AM. Science and technology for water purification in the coming decades. Nature 2008;452:301–10.
[2] Sharon H, Reddy KS. A review of solar energy driven desalination technologies. Renew Sustain Energy Rev 2015;41:1080–118.
[3] Ward J. A plastic solar water purifier with high output. Sol Energy 2003;75:433–7.
[4] Zurigat YH, Abu-Arabi MK. Modelling and performance analysis of a regenerative solar desalination unit. Appl Therm Eng 2004;24:1061–72.
[5] Al-Hayeka I, Badran OO. The effect of using different designs of solar stills on water distillation. Desalination 2004;169:121–7.
[6] Karimi Estahbanati MR, Ahsan A, Feilizadeh M, Jafarpur K, Ashrafmansouri S-S, Feilizadeh M. Theoretical and experimental investigation on internal reflectors in a single-slope solar still. Appl Energy 2016;165:537–47.
[7] Badran AA, Al-Hallaq IA, Eyal Salman IA, Odat MZ. A solar still augmented with a flat-plate collector. Desalination 2005;172:227–34.
[8] Tiris C, Tiris M, Erdalli Y, Sohmen M. Experimental studies on a solar still coupled with a flat-plate collector and a single basin still. Energy Convers Manage 1998;39:853–6.
[9] Mohamad MA, Soliman SH, Abdel-Salam MS, Hussein HMS. Experimental and financial investigation of asymmetrical solar stills with different insulation. Appl Energy 1995;52(2–3):265–71.
[10] Minasian AN, Al-Karaghouli AA. An improved solar still: the wick-basin type. Energy Convers Manage 1995;36:213–7.
[11] El-Sebaii AA. Thermal performance of a triple-basin solar still. Desalination 2005;174:23–37.
[12] Bouchekima B. A small solar desalination plant for the production of drinking water in remote arid areas of southern Algeria. Desalination 2003;159:197–204.
[13] Karimi Estahbanati MR, Feilizadeh M, Jafarpur K, Feilizadeh M, Rahimpour MR. Experimental investigation of a multi-effect active solar still: the effect of the number of stages. Appl Energy 2015;137:46–55.
[14] Voropoulos K, Mathioulakis E, Belessiotis V. Solar stills coupled with solar collectors and storage tank-–analytical simulation and experimental validation of energy behavior. Sol Energy 2003;75:199–205.
[15] Bhardwaj R, ten Kortenaar MV, Mudde RF. Maximized production of water by increasing area of condensation surface for solar distillation. Appl Energy 2015;154:480–90.
[16] Nafey AS, Abdelkader M, Abdelmotalip A, Mabrouk AA. Solar still productivity enhancement. Energy Convers Manage 2001;42:1401–8.
[17] Dutt DK. Performance of a double-basin solar still in the presence of dye. Appl Energy 1989;32:207–23.
[18] Abu-Hijleh BAK, Rababa'h HM. Experimental study of a solar still with sponge cubes in basin. Energy Convers Manage 2003;44:1411–8.
[19] Al-Karaghouli AA, Al Naser WE. Experimental comparative study of the double basin solar stills. Appl Energy 2004;77:317–25.
[20] Tiwari GN, Singh HN, Tripathi R. Present status of solar distillation. Sol Energy 2003;75:367–73.
[21] El-Sebaii AA, Aboul-Enein S, El-Bialy E. Single basin solar still with baffle suspended absorber. Energy Convers Manage 2000;41:661–75.
[22] Kalidasa Murugavel K, Chockalingam KKSK, Srithar K. An experimental study on single basin double slope simulation solar still with thin layer of water in the basin. Desalination 2008;220:687–93.
[23] Kalidasa Murugavel K, Sivakumar S, Riaz Ahamed J, Chockalingam KKSK, Srithar K. Single basin double slope solar still with minimum basin depth and energy storing materials. Appl Energy 2010;87:514–23.
[24] Kumar S, Tiwari GN. Life cycle cost analysis of single slope hybrid (PV/T) active solar still. Appl Energy 2009;86:1995–2004.
[25] Abdullah AS. Improving the performance of stepped solar still. Desalination 2013;319:60–5.
[26] Morad MM, El-Maghawry HAM, Wasfy KI. Improving the double slope solar still performance by using flat-plate solar collector and cooling glass cover. Desalination 2015;373:1–9.
[27] Xiao G, Wang X, Ni M, Wang F, Zhu W, Luo Z, et al. A review on solar stills for brine desalination. Appl Energy 2013;103:642–52.

[28] El-Samadony YAF, Kabeel AE. Theoretical estimation of the optimum glass cover water film cooling parameters combinations of a stepped solar still. Energy 2014;68:744–50.
[29] Gude VG. Energy storage for desalination processes powered by renewable energy and waste heat sources. Appl Energy 2015;137:877–98.
[30] Tabrizi FF, Dashtban M, Moghaddam H. Experimental investigation of a weir-type cascade solar still with built-in latent heat thermal energy storage system. Desalination 2010;260:248–53.
[31] Dashtban M, Tabrizi FF. Thermal analysis of a weir-type cascade solar still integrated with PCM storage. Desalination 2011;279:415–22.
[32] Ansari O, Asbik M, Bah A, Arbaoui A, Khmou A. Desalination of the brackish water using a passive solar still with a heat energy storage system. Desalination 2013;324:10–20.
[33] Ghozatloo A, Rashidi A, Shariaty-Niassar M. Convective heat transfer enhancement of graphene nanofluids in shell and tube heat exchanger. Exp Thermal Fluid Sci 2014;53:136–41.
[34] Yu W, Xie H. A review on nanofluids: preparation, stability mechanisms, and applications. J Nanomater 2012;2012:1–17.
[35] Mehrali M, Sadeghinezhad E, Latibari ST, Kazi SN, Mehrali M, Zubir MNBM, et al. Investigation of thermal conductivity and rheological properties of nanofluids containing graphene nanoplatelets. Nanoscale Res Lett 2014;9:1–12.
[36] Sharshir SW, Yang N, Peng G, Kabeel AE. Factors affecting solar stills productivity and improvement techniques: a detailed review. Appl Therm Eng 2016;100:267–84.
[37] Owolabi Afolabi L, Al-Kayiem Hussain H, Baheta Aklilu T. Nanoadditives induced enhancement properties of paraffin-based nanocomposites for thermal energy storage. Sol Energy 2016;135:644–53.
[38] Lin SC, Al-Kayiem HH. Evaluation of copper nanoparticles – paraffin wax compositions for solar thermal energy storage. Sol Energy 2016;132:267–78.
[39] Murshed SMS, Nieto de Castro CA. Conduction and convection heat transfer characteristics of ethylene glycol based nanofluids – a review. Appl Energy 2016;184:681–95.
[40] Yang Y, Zhang ZG, Grulke EA, Anderson WB, Wu G. Heat transfer properties of nanoparticle-in-fluid dispersions (nanofluids) in laminar flow. Int J Heat Mass Transf 2005;48:1107–16.
[41] Sharshir SW, Peng G, Wu L, Yang N, Essa FA, Elsheikh AH, et al. Enhancing the solar still performance using nanofluids and glass cover cooling: experimental study. Appl Therm Eng 2017;113:684–93.
[42] Nijmeh S, Odeh S, Akash B. Experimental and theoretical study of a single-basin solar sill in Jordan. Int Commun Heat Mass Transfer 2005;32:565–72.
[43] Elango T, Kannan A, Kalidasa Murugavel K. Performance study on single basin single slope solar still with different water nanofluids. Desalination 2015;360:45–51.
[44] Kabeel AE, Omara ZM, Essa FA. Enhancement of modified solar still integrated with external condenser using nanofluids: an experimental approach. Energy Convers Manage 2014;78:493–8.
[45] Sahota L, Tiwari GN. Effect of $Al_2O_3$ nanoparticles on the performance of passive double slope solar still. Sol Energy 2016;130:260–72.
[46] Suganthi KS, Vinodhan V Leela, Rajan KS. Heat transfer performance and transport properties of ZnO–ethylene glycol and ZnO–ethylene glycol–water nanofluid coolants. Appl Energy 2014;135:548–59.
[47] Wang JJ, Zheng RT, Gao JW, Chen G. Heat conduction mechanisms in nanofluids and suspensions. Nano Today 2012;7:124–36.
[48] Persad AH, Ward CA. Expressions for the evaporation and condensation coefficients in the hertz-Knudsen relation. Chem Rev 2016;116:7727–67.
[49] Tso CY, Chao CYH. Study of enthalpy of evaporation, saturated vapor pressure and evaporation rate of aqueous nanofluids. Int J Heat Mass Transf 2015;84:931–41.
[50] Huang Z, Li X, Yuan H, Feng Y, Zhang X. Hydrophobically modified nanoparticle suspensions to enhance water evaporation rate. Appl Phys Lett 2016;109:161602.